



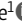






## COMMUNICATION

# Exercise training may reduce fragmented mitochondria in the ischemic-reperfused heart through DRP1

Mathilde Dubois<sup>1</sup>, Florian Pallot<sup>1\*</sup>, Maxime Gouin-Gravezat<sup>1\*</sup>, Doria Boulghobra<sup>1\*</sup>, Florence Coste<sup>1</sup>, Guillaume Walther<sup>1</sup>, Gregory Meyer<sup>1</sup>, Isabelle Bornard<sup>2</sup>, and Cyril Reboul<sup>1</sup>

**Mitochondrial fission is a key trigger of cardiac ischemia-reperfusion injuries (IR). Exercise training is an efficient cardioprotective strategy, but its impact on mitochondrial fragmentation during IR remains unknown. Using isolated rat hearts, we found that exercise training limited the activation of dynamin-like protein 1 and limited mitochondrial fragmentation during IR. These results support the hypothesis that exercise training contributes to cardioprotection through its capacity to modulate the mitochondrial fragmentation during IR.**

## Introduction

Acute myocardial infarction is a leading cause of death worldwide. Reperfusion of the ischemic area is the current standard therapy. However, it results in important heart cell dysfunctions known as ischemic reperfusion (IR) injuries. In the past decade, the key role of mitochondria in IR injuries has been highlighted (Kuznetsov et al., 2019). During early reperfusion, mitochondrial network disruption, defined as the imbalance between mitochondrial fusion and fission, has emerged as a new relevant factor to explain the heart's vulnerability to IR (Maneechote et al., 2017). Indeed, inhibition of cardiac mitochondrial fission during IR using mitochondrial division inhibitor-1 (mdivi-1) delays the opening of the mitochondrial permeability transition pore (mPTP), limits mitochondrial ROS overproduction (Ding et al., 2022), and reduces infarct size (Ong et al., 2010).

Among the strategies known to reduce IR injuries, physical activity has been much studied (Farah et al., 2013). Recently, we (Boulghobra et al., 2021) and others (Lee et al., 2012) reported that the cardioprotective effect of exercise training (ExTr) could be explained by its impact on mitochondrial ROS production and mPTP activation during early reperfusion. It was previously reported that mitochondrial fission is a normal heart response to increased energy demand during exercise (Coronado et al., 2018). Conversely, it is not known whether ExTr can influence the mitochondrial network during IR. To the best of our knowledge, only one study focused on ExTr effect on the mitochondrial network during IR (Ghahremani et al., 2018). However, as this study only

monitored the gene expression level of proteins involved in mitochondrial fission regulation, the results are inconclusive.

Therefore, we investigated whether ExTr in rats modulate IR deleterious impact on the mitochondrial network during early reperfusion, known as a critical period determining the severity of reperfusion lesions. Using western blotting and transmission electron microscopy, we reported for the first time that ExTr resulted in less fragmented mitochondria during early post-IR.

## Materials and methods

### Animal model

All animal experiments were performed according to the European Parliament Directive 2010/63/EU and were approved by the local ethics committee (No. CEEA-00223, #27001). Male Wistar rats (12-wk-old; weight = 225–275 g, Janvier) were randomly assigned to a sedentary control group (Sed) or a 5-wk ExTr group, as previously described (Farah et al., 2013). Moderate ExTr was performed according to a protocol previously described to reduce heart vulnerability to IR (Farah et al., 2013). Briefly, rats exercised on a motor-driven treadmill (47300; Ugo Basile) 45 min/day, 5 days/wk for 5 wk at 25 m/min (≈60% of their MAV). To avoid the acute effects of exercise, 17-wk-old rats were sacrificed 24 h after the last ExTr session.

<sup>1</sup>LAPEC UPR-4278, Avignon Université, Avignon, France; <sup>2</sup>UR407 INRAE Pathologie Végétale, INRAE, Avignon, France.

\*F. Pallot, M. Gouin-Gravezat, and D. Boulghobra contributed equally to this paper. Correspondence to Cyril Reboul: [cyril.reboul@univ-avignon.fr](mailto:cyril.reboul@univ-avignon.fr).

© 2024 Dubois et al. This article is distributed under the terms of an Attribution–Noncommercial–Share Alike–No Mirror Sites license for the first six months after the publication date (see <http://www.rupress.org/terms/>). After six months it is available under a Creative Commons License (Attribution–Noncommercial–Share Alike 4.0 International license, as described at <https://creativecommons.org/licenses/by-nc-sa/4.0/>).

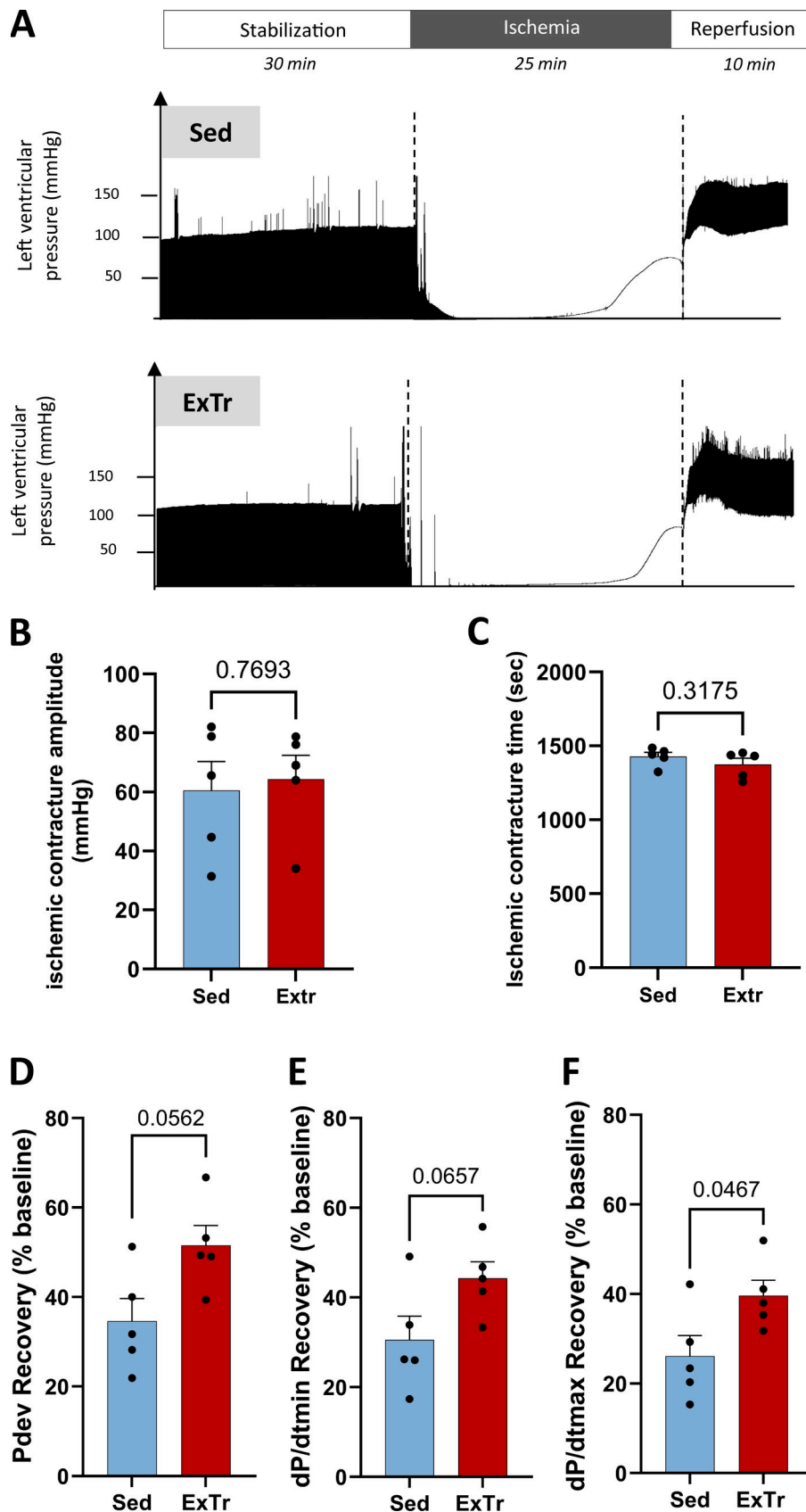


**Figure 1. Effect of ExTr on left ventricular heart function after IR. (A–F)** Schematic illustration of the experimental protocol (upper panel). Hearts from sedentary (Sed,  $n = 5$ ) and exercised (ExTr,  $n = 5$ ) rats were stabilized for 30 min using a Langendorff apparatus. Then, hearts underwent a total no-flow ischemia for 25 min followed by 10 min of reperfusion. Left ventricular (LV) pressure traces in the hearts of Sed (middle) and ExTr rats (lower panel) during the IR protocol. Ischemic contracture time (B) and maximal ischemic contracture amplitude (C) in isolated hearts from Sed and ExTr rats undergoing ex vivo IR. Recovery of LV developed pressure (Pdev) (D), minimal (E), and maximal (F) first derivative pressure (dP/dtmin and dP/dtmax, respectively) after 10 min of post-IR. ExTr versus Sed P-value obtained with non-parametric  $t$  test. Data are mean  $\pm$  SEM.

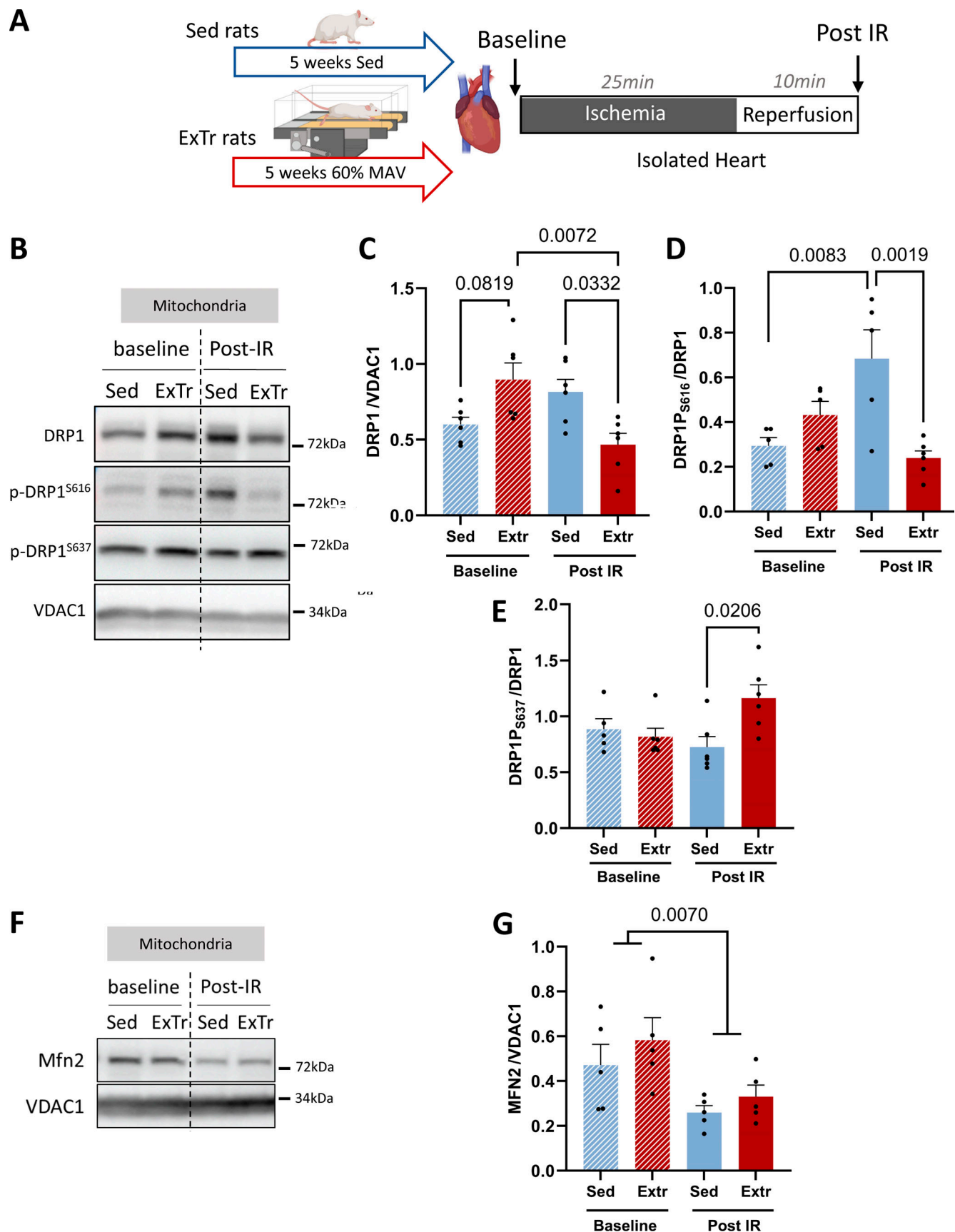


Figure 2. **Effect of ExTr on Drp1 signaling pathway in basal condition and after ex vivo IR.** (A) Schematic illustration of the experimental protocol. Hearts from sedentary (Sed,  $n = 12$ ) and exercised (ExTr,  $n = 12$ ) rats underwent or did not undergo an IR ex vivo. Western blotting was performed on hearts before

(baseline) or after IR (post IR). **(B)** Representative western blots showing phosphorylated DRP1 (p-DRP1<sup>Ser616</sup> and p-DRP1<sup>Ser637</sup>) and total DRP1 expression level in the mitochondrial subfraction of Sed and ExTr hearts, in basal condition (baseline) or after ex vivo IR (Post-IR). **(C–E)** Quantification of total DRP1 and DRP1 phosphorylated at Ser616 and Ser637 in mitochondrial subfractions analyzed by western blotting in hearts from Sed and ExTr rats, in basal condition (baseline,  $n = 5$ –6 hearts in duplicate), or after ex vivo IR (Post-IR,  $n = 6$  hearts in duplicate). DRP1 level was expressed relative to VDAC1 in mitochondria samples. Sed versus ExTr  $p$ -value obtained with two-way ANOVA followed by Tukey's multiple comparisons test; Data are mean  $\pm$  SEM. **(F)** Representative western blots showing Mfn2 expression level in the mitochondrial subfraction of Sed and ExTr hearts, in basal condition (baseline), or after ex vivo IR (Post-IR). **(G)** Quantification of Mfn2 in mitochondrial subfractions analyzed by western blotting in hearts from Sed and ExTr rats that underwent (Post-IR;  $n = 6$  hearts in duplicate) or did not undergo (baseline;  $n = 5$  hearts in duplicate) IR. Mfn2 level was expressed relative to VDAC1 in mitochondria samples. Sed versus ExTr  $P$ -value obtained with two-way ANOVA followed by Tukey's multiple comparisons test. Data are mean  $\pm$  SEM. Source data are available for this figure: SourceData F2.

### IR on isolated perfused hearts

IR was performed on a Langendorff apparatus, as previously described (Dubois et al., 2024). Briefly, after stabilization, a total no-flow ischemia was performed for 25 min followed by 10 min of reperfusion. The left ventricular (LV) pressure (MP36R; BioPac System Inc.) was recorded during the entire perfusion and the cardiac functional recovery following IR was determined. LV ischemic contracture time and amplitude were measured at the peak of contracture during ischemia. LV tissues were flash-frozen in liquid nitrogen for biochemical experiments or fixed in 2.5% glutaraldehyde/2% paraformaldehyde in a sodium cacodylate buffer (0.1 M) for electron microscopy analysis.

### Western blotting

Western blotting was performed on the LV free wall as previously described (Boulghobra et al., 2021). Hearts were removed either directly after the 5 wk of training (baseline) or after an ex vivo IR procedure on an isolated perfused heart (post IR), as illustrated in Fig. 2 A. Mitochondrial proteins were separated on polyacrylamide-SDS gels and transferred to PVDF membranes. Membranes were blocked and then incubated at 4°C with primary antibodies against dynamin-related protein 1 (Drp1) (1:1,000; Cell Signaling), P-Drp1 S616 (1:500; Cell Signaling), P-Drp1 S637 (1:1,000; Cell Signaling), Mfn2 (1:1,000; Santa Cruz Biotechnology), and VDAC1 (1:5,000; Thermo Fisher Scientific). As a mitochondrial subfraction, VDAC1 was used as a housekeeping protein. The corresponding HRP-conjugated IgG (secondary antibodies) was used according to standard procedures. Immunodetection and revelation were carried out using the ECL chemiluminescence system (VILBER Fusion FX) (Table S1).

### Transmission electron microscopy

Hearts were removed either directly after 5 wk of training (baseline) or after an ex vivo IR procedure on an isolated perfused heart (post IR), as shown in Fig. 3, A and G. Samples of the subendocardial layer of the LV free wall were washed and fixed in 2.5% glutaraldehyde/2% paraformaldehyde in 0.1 M sodium cacodylate buffer. After rinsing, samples were post-fixed in 1% osmium tetroxide for 1 h, dehydrated through a graded ethanol series, and embedded in resin. Ultrathin heart tissue sections were prepared with a diamond knife and a Reichert Ultracut E ultramicrotome and stained with uranyl acetate and lead citrate. Images were acquired using a transmission electron microscope (TEM-Hitachi H7800) by randomly selecting areas of longitudinally arranged cardiomyocytes.

### Statistical analyses

Data were expressed as the mean  $\pm$  SEM or as the median and interquartile range for the violin plots. The normal distribution of the data was tested with the Shapiro–Wilk normality test. Experimental conditions were compared with Student's  $t$  test, analysis of variance (ANOVA) followed by Tukey's multiple comparisons test, nested analysis of variance (ANOVA), or nested  $t$  test. When necessary, non-parametric tests were used (Mann–Whitney test for two groups). A  $P < 0.05$  value was considered statistically significant. The  $P$ -value was reported in all graphs. Statistical analyses were done with GraphPad Prism (8.4.3).

### Online supplemental material

Materials and methods are described in detail in the supplemental text at the end of the PDF. A table summarizing the conditions of antibody use for the biochemical analysis is available in the supplemental text at the end of the PDF and in Table S1.

## Results and discussion

To evaluate the impact of ExTr on mitochondrial fission during cardiac IR, we first confirmed the cardioprotective effect of 5 wk of ExTr on heart vulnerability to IR. To this aim, we performed global ischemia followed by reperfusion on isolated perfused hearts (Langendorff apparatus) from Sed and ExTr rats. No impact of ExTr was reported regarding the onset of ischemic contracture (Fig. 1 B) and its amplitude (Fig. 1 C). However, as previously reported by our group (Farah et al., 2013) and others (Bowles et al., 1992), ExTr improved IR cardiac functional recovery (Fig. 1, D–F), as indicated by the higher LV developed pressure (Pdev; Fig. 1 D) and LV contractility indexes (Fig. 1, E and F). In addition, using exactly the same protocol (ExTr intensity and duration), we previously showed that this functional recovery improvement during early reperfusion is associated with reduced ROS production and infarct size (Farah et al., 2013). Alterations of the mitochondrial fusion/fission equilibrium have been well described to play a key role in heart sensitivity to IR (Maneechote et al., 2017). In addition, it has been well described that the GTPase DRP1 plays a key role in excessive mitochondrial fragmentation that occurs during IR (Ong et al., 2010). Considering this, we next evaluated the impact of 5 wk of ExTr on DRP1 level in the mitochondrial subfraction and on its phosphorylation level (Fig. 2, A–E). We reported a trend toward increasing DRP1 levels in the mitochondrial subfraction of ExTr hearts compared with Sed ones ( $P = 0.0819$ ) (Fig. 2 C). No changes were reported regarding the phosphorylation of DRP1



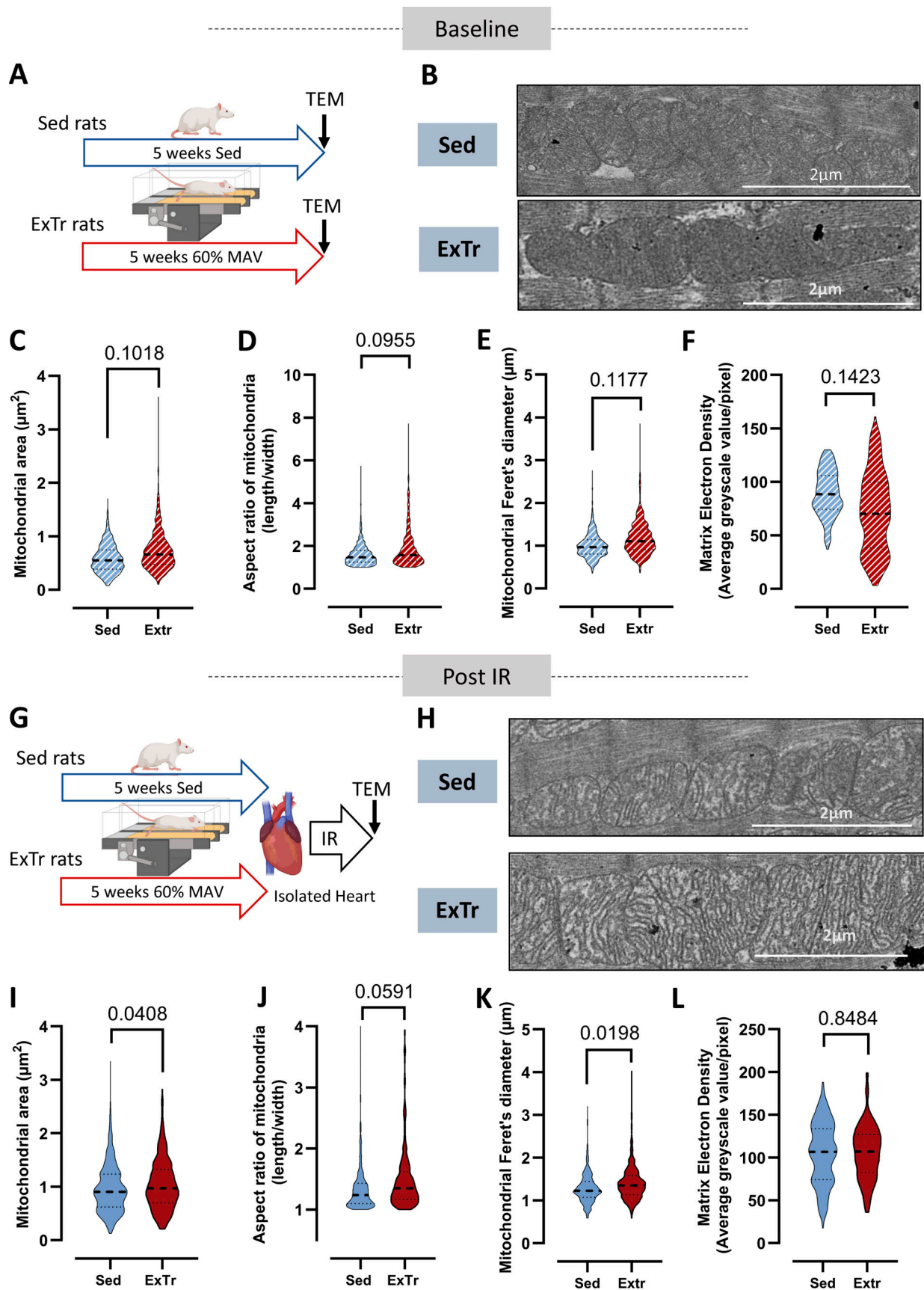


Figure 3. **Effect of ExTr on mitochondrial shape in basal condition and after ex vivo IR.** (A) Schematic illustration of the experimental protocol. Transmission electron microscopy was performed in the hearts of sedentary (Sed,  $n = 3$ ) and 5-wk-exercised (ExTr,  $n = 3$ ) rats. (B–F) Representative

transmission electron microscopy images of cardiac mitochondria from Sed and ExTr hearts (Baseline). Quantification of the mitochondrial area (C), aspect ratio (D), Feret's diameter (E), and matrix electron density (F) of hearts from Sed or ExTr rats. (G) Schematic illustration of the experimental protocol. Transmission electron microscopy was performed in the hearts of sedentary (Sed,  $n = 3$ ) and 5-wk-exercised (ExTr,  $n = 3$ ) rats after an ex vivo IR. (H-L) Representative transmission electron microscopy images of cardiac mitochondria from Sed and ExTr hearts after IR (Post-IR). Quantification of the mitochondrial area (I), aspect ratio (J), Feret's diameter (K), and matrix electron density (L) of hearts from Sed or ExTr rats that underwent IR. The mitochondrial shape was measured in ~600–750 mitochondria from three independent hearts in each condition. Sed versus ExTr P-value obtained with nested  $t$  test. Data are median and interquartile range. Source data are available for this figure: SourceData F3.

both on its main activation site (Ser616, Fig. 2 D) and its inhibitory site (Ser637, Fig. 2 E) in basal conditions. Following ischemia (25 min) and early reperfusion (10 min), known as a critical period determining the severity of reperfusion lesions, the level of DRP1 in the mitochondrial subfraction was increased by 36% in Sed hearts, without reaching statistical significance, and, at the opposite, was significantly decreased by 48% in ExTr hearts (Fig. 2, B and C). Thus, during early reperfusion, the expression level of DRP1 was lower in the mitochondrial subfraction of ExTr hearts compared with Sed ones (Fig. 2, B and C). In addition, we also reported that following IR, the phosphorylation of DRP1 on Ser616 was markedly increased in the Sed hearts, whereas no effect was reported in ExTr animals (Fig. 2, B and D). As a consequence, during early reperfusion, this parameter was lower in ExTr hearts compared with Sed ones (Fig. 2, B and D). Regarding the phosphorylation of DRP1 on its inhibitory site (Ser637), we did not observe a significant impact of IR in Sed hearts but we reported that in the ExTr hearts, the phosphorylation on Ser637 tended to be increased ( $P = 0.0805$ ) (Fig. 2, B and E). Then, at the time of early reperfusion, the phosphorylation on Ser637 was significantly higher in the mitochondrial subfraction of ExTr hearts compared to Sed ones (Fig. 2, B and E). Altogether, these results support a lower activation state of DRP1 in the mitochondrial subfraction of ExTr hearts compared with Sed ones during early reperfusion. Previous work reported that ExTr results in a higher level of Mitofusin2 (MFN2) mRNA following IR (Ghahremani et al., 2018). Considering that MFN2 overexpression is associated with cardioprotection (Xiong et al., 2019) and that MFN2 is known as a central regulator of mitochondrial fusion, we next asked whether ExTr could influence the expression level of MFN2 in mitochondrial subfraction following 5 wk of ExTr and during early post-IR. We reported that IR was associated with a decrease in the expression level of MFN2 without a specific impact on our experimental groups (Fig. 2, F and G). Indeed, when compared with Sed hearts, no impact of ExTr was reported on the mitochondrial level of MFN2 in baseline condition as well as during early reperfusion (Fig. 2, F and G).

Considering these results obtained on key signaling pathways involved in the regulation of mitochondrial fission/fusion equilibrium, we next investigated the consequences of our experimental conditions on mitochondrial shape by transmission electron microscopy (Fig. 3, A and B). Following 5 wk of ExTr, we reported that although mitochondrial area (Fig. 3 C), aspect ratio (Fig. 3 D), and Feret's diameter (Fig. 3 E), three different indexes of mitochondrial fusion/fission equilibrium, tended to be higher when compared with sedentary hearts, no significant difference was reported for these three parameters. We also reported that the matrix electron

density, an index of mitochondrial cristae density for which denser areas (higher cristae density) appear with lower grayscale values (Allen et al., 2020), tended to be lower in ExTr hearts compared with Sed ones (Fig. 3 F). This suggests higher mitochondrial cristae density following 4 wk of ExTr. Together, these results highlight that mitochondria only tended to be more fused in ExTr hearts with a trend toward higher cristae density. In the literature, the impact of ExTr on cardiac mitochondrial shape remain controversial. Indeed, only the work of Guski et al. (1980) reported that following 45 h of ExTr, both mitochondrial volume and cristae density were increased. Regarding the size of mitochondria, some studies reported that following ExTr (4 wk), the size of the mitochondria was reduced (Jia et al., 2019) whereas others reported some positive impact of ExTr (12 wk) (Yuan et al., 2021), suggesting a potential impact of ExTr duration.

Considering the impact of ExTr on DRP1 activation during IR (Fig. 2), we next evaluated the impact of myocardial IR. Using nested ANOVA analyses, we reported some significant impact of IR on the mitochondrial area (Sed: +66%,  $P = 0.0002$ ; ExTr: +44%,  $P = 0.0008$ ) and Feret's diameter (Sed: +21%,  $P = 0.0147$ ; ExTr: +15%,  $P = 0.0434$ ) both in Sed and ExTr hearts. We also reported a trend toward a decrease of the aspect ratio in Sed hearts (–15%,  $P = 0.1020$ ) and a significant decrease of this index in the ExTr hearts (–21%,  $P = 0.0150$ ). Finally, we reported that matrix electron density was increased by 16% in Sed hearts, without reaching statistical significance, and by 49% in ExTr hearts ( $P = 0.018$ ). These results, suggesting mitochondrial swelling and fragmentation during IR in both Sed and ExTr hearts, must be taken cautiously. Indeed, the TEM images of baseline conditions were obtained from hearts fixed directly after the euthanasia of the animals, while IR hearts were perfused with Krebs-Henseleit buffer on a Langendorff apparatus before being fixed. Then, mitochondrial swelling, which is a classic feature of IR, may also have been affected by Krebs-Henseleit buffer perfusion, known to induce myocardial edema independently of IR (Andrés-Villarreal et al., 2016). Such phenomenon can also impact mitochondrial structure due to osmotic stress and intracellular water content. Considering this, in Fig. 3, we choose to compare results obtained on mitochondrial shape during reperfusion independently to those obtained under basal conditions. We reported that mitochondrial area was higher in ExTr hearts than Sed ones during early reperfusion (Fig. 3 I). This parameter is strongly influenced both by mitochondrial fragmentation and swelling. Considering that there is an inverse relationship between mitochondrial cristae density and mitochondrial swelling, we next measured matrix electron density as an index of cristae density and we did not observe any difference between groups during early reperfusion (Fig. 3 L), suggesting comparable mitochondrial swollen state in Sed and ExTr hearts during early reperfusion. These results are

not in accordance with studies showing that ExTr limits the activation of mPTP (Boulghobra et al., 2021), and further studies on the reversibility of such mitochondrial swelling observed during early reperfusion would be necessary. Considering these results suggesting that the mitochondria of the ExTr hearts were less fragmented than the Sed ones, we next studied both the mitochondrial aspect ratio (Fig. 3 J) and Feret's diameter (Fig. 3 K) as indexes of mitochondrial fragmentation. We reported that mitochondrial the aspect ratio tended to be higher in the ExTr compared with Sed hearts ( $P = 0.0591$ ) and that the Feret's diameter was higher in the ExTr hearts compared with Sed ones (Fig. 3, J and K), confirming that during early reperfusion, mitochondria of the ExTr hearts were less fragmented than mitochondria of Sed hearts. In addition, we also observed more elongated mitochondria in ExTr than Sed hearts after IR. These results could be explained by the lower activation of DRP1 we reported in Fig. 2, B–E in response to IR and could support the hypothesis that the ExTr heart is more able to preserve a fused state of these mitochondria during IR. Indeed, the role of DRP1 activation and translocation to mitochondria in the severity of IR injuries has been well described (Ong et al., 2010). Most studies show that Ser616 phosphorylation promotes the translocation of Drp1 to the mitochondrial outer membrane, whereas Ser637 phosphorylation reverses this process (Tong et al., 2020). It is well described that both  $\text{Ca}^{2+}$  and ROS-dependent kinases, such as CaMKII, regulate DRP1Ser616 phosphorylation. This could contribute to explaining that the level Ser616 phosphorylation was higher during IR (Wang et al., 2022). Thus, we could hypothesize here that in the ExTr hearts, the better regulation of  $\text{Ca}^{2+}$  homeostasis and the lower level of ROS production during IR (Boulghobra et al., 2020) contribute to limiting the activation of such kinases and then the activation of DRP1. Regarding the phosphorylation on Ser637, it is well described that the calcium-dependent phosphatase calcineurin dephosphorylates this specific inhibitory site of DRP1, which promotes its recruitment to mitochondria (Cribbs and Strack, 2007). Interestingly, this phosphatase is also known to be ROS-sensitive (DeGrande et al., 2013). The same hypothesis could then be advanced to explain that ExTr modulates the phosphorylation of DRP1 on Ser637 during IR. Further studies are needed to better understand the impact of ExTr on DRP1 regulation during myocardial infarction and its role in exercise-induced cardioprotection.

### Study limitation

This study has some limitations. The main limitation concerns the difficulty of measuring the dynamic equilibrium between mitochondrial fusion and fission in cardiac tissue. Considering this, we discussed rather about the fragmented state of the mitochondria measured at a given time than mitochondrial fission or fusion. In addition, it is well known that mitochondrial interactions are complex and that the longitudinal 2-D evaluation of this network does not reveal its full complexity. Further studies using 3-D reconstruction of the mitochondrial network following IR in Sed and ExTr hearts will be necessary to better understand the impact of exercise-induced cardioprotection. Another limitation of the present work concerns the fact that myocardial IR was performed on isolated hearts perfused with a

crystalloid solution that could impact osmotic equilibrium and then the mitochondrial shape. For this reason, data obtained in baseline conditions (non-crystalloid perfused hearts) and following IR (crystalloid perfused hearts) were treated independently. To better understand the direct impact of IR on cardiac mitochondrial shape in ExTr hearts, further in vivo IR experiments will be necessary. Another limitation of the present work concerns the difficulty of concluding the role of lower mitochondrial fragmentation on the cardioprotective impact of ExTr. Indeed, although it has been well described that the inhibition of excessive mitochondrial fragmentation during cardiac IR results in less severe injuries (Maneechote et al., 2017), further studies are necessary to decipher the potential key role of this phenomenon in exercise-induced cardioprotection.

### Conclusion

In conclusion, these results support the hypothesis that ExTr limits the activation of DRP1 during early post-IR which is associated with less fragmented mitochondria. As excessive mitochondrial fission is considered a key trigger of IR injuries, our findings could contribute to understanding how exercise protects the heart during IR. However, more studies are necessary to determine whether this phenomenon constitutes or not a key trigger of exercise-induced cardioprotection.

### Data availability

All data are available from the corresponding authors upon reasonable request.

### Acknowledgments

David A. Eisner served as the editor.

The authors thank Christine Bothuan for technical assistance at the animal facility.

Author contributions: M. Dubois: Conceptualization, Data curation, Formal analysis, Investigation, Methodology, Project administration, Validation, Visualization, Writing - original draft, Writing - review & editing, F. Pallot: Data curation, Formal analysis, Investigation, Writing - review & editing, M. Gouin-Gravezat: Data curation, Investigation, Methodology, Visualization, Writing - review & editing, D. Boulghobra: Investigation, Methodology, Writing - original draft, F. Coste: Conceptualization, Writing - review & editing, G. Walther: Conceptualization, Methodology, G. Meyer: Conceptualization, Methodology, Writing - review & editing, I. Bornard: Resources, C. Reboul: Conceptualization, Data curation, Formal analysis, Funding acquisition, Investigation, Methodology, Project administration, Supervision, Validation, Writing - original draft, Writing - review & editing.

Disclosures: The authors declare no competing interests exist.

Submitted: 13 September 2023

Revised: 16 July 2024

Revised: 9 September 2024

Revised: 25 September 2024

Accepted: 7 October 2024



## References

- Allen, M.E., E.R. Pennington, J.B. Perry, S. Dadoo, M. Makrecka-Kuka, M. Dambrova, F. Moukdar, H.D. Patel, X. Han, G.K. Kidd, et al. 2020. The cardiolipin-binding peptide elamipretide mitigates fragmentation of cristae networks following cardiac ischemia reperfusion in rats. *Commun. Biol.* 3:389. <https://doi.org/10.1038/s42003-020-1101-3>
- Andrés-Villarreal, M., I. Barba, M. Poncelas, J. Inserte, J. Rodriguez-Palmares, V. Pineda, and D. Garcia-Dorado. 2016. Measuring water distribution in the heart: Preventing edema reduces ischemia-reperfusion injury. *J. Am. Heart Assoc.* 5:e003843. <https://doi.org/10.1161/JAHA.116.003843>
- Boulghobra, D., F. Coste, B. Geny, and C. Reboul. 2020. Exercise training protects the heart against ischemia-reperfusion injury: A central role for mitochondria? *Free Radic. Biol. Med.* 152:395–410. <https://doi.org/10.1016/j.freeradbiomed.2020.04.005>
- Boulghobra, D., M. Dubois, B. Alpha-Bazin, F. Coste, M. Olmos, S. Gayrard, I. Bornard, G. Meyer, J.-C. Gaillard, J. Armengaud, and C. Reboul. 2021. Increased protein S-nitrosylation in mitochondria: A key mechanism of exercise-induced cardioprotection. *Basic Res. Cardiol.* 116:66. <https://doi.org/10.1007/s00395-021-00906-3>
- Bowles, D.K., R.P. Farrar, and J.W. Starnes. 1992. Exercise training improves cardiac function after ischemia in the isolated, working rat heart. *Am. J. Physiol.* 263:H804–H809. <https://doi.org/10.1152/ajpheart.1992.263.3.H804>
- Coronado, M., G. Fajardo, K. Nguyen, M. Zhao, K. Kooiker, G. Jung, D.-Q. Hu, S. Reddy, E. Sandoval, A. Stotland, et al. 2018. Physiological mitochondrial fragmentation is a normal cardiac adaptation to increased energy demand. *Circ. Res.* 122:282–295. <https://doi.org/10.1161/CIRCRESAHA.117.310725>
- Cribbs, J.T., and S. Strack. 2007. Reversible phosphorylation of Drp1 by cyclic AMP-dependent protein kinase and calcineurin regulates mitochondrial fission and cell death. *EMBO Rep.* 8:939–944. <https://doi.org/10.1038/sj.embor.7401062>
- DeGrande, S.T., S.C. Little, D.J. Nixon, P. Wright, J. Snyder, W. Dun, N. Murphy, A. Kilic, R. Higgins, P.F. Binkley, et al. 2013. Molecular mechanisms underlying cardiac protein phosphatase 2A regulation in heart. *J. Biol. Chem.* 288:1032–1046. <https://doi.org/10.1074/jbc.M112.426957>
- Ding, J., Z. Zhang, S. Li, W. Wang, T. Du, Q. Fang, Y. Wang, and D.W. Wang. 2022. Mdivi-1 alleviates cardiac fibrosis post myocardial infarction at infarcted border zone, possibly via inhibition of Drp1-Activated mitochondrial fission and oxidative stress. *Arch. Biochem. Biophys.* 718: 109147. <https://doi.org/10.1016/j.abb.2022.109147>
- Dubois, M., D. Boulghobra, G. Rochebloine, F. Pallot, M. Yehya, I. Bornard, S. Gayrard, F. Coste, G. Walther, G. Meyer, et al. 2024. Hyperglycemia triggers RyR2-dependent alterations of mitochondrial calcium homeostasis in response to cardiac ischemia-reperfusion: Key role of DRP1 activation. *Redox Biol.* 70:103044. <https://doi.org/10.1016/j.redox.2024.103044>
- Farah, C., A. Kleindienst, G. Bolea, G. Meyer, S. Gayrard, B. Geny, P. Obert, O. Cazorla, S. Tanguy, and C. Reboul. 2013. Exercise-induced cardioprotection: A role for eNOS uncoupling and NO metabolites. *Basic Res. Cardiol.* 108:389. <https://doi.org/10.1007/s00395-013-0389-2>
- Ghahremani, R., A. Damirchi, I. Salehi, A. Komaki, and F. Esposito. 2018. Mitochondrial dynamics as an underlying mechanism involved in aerobic exercise training-induced cardioprotection against ischemia-reperfusion injury. *Life Sci.* 213:102–108. <https://doi.org/10.1016/j.lfs.2018.10.035>
- Guski, H., G. Wassilew, and R. Meyer. 1980. Ultrastructural morphometric studies of mitochondrial membranes in the rat heart after physical training. *Exp. Pathol. (Jena)*. 18:510–519. [https://doi.org/10.1016/S0014-4908\(80\)80009-3](https://doi.org/10.1016/S0014-4908(80)80009-3)
- Jia, D., L. Hou, Y. Lv, L. Xi, and Z. Tian. 2019. Postinfarction exercise training alleviates cardiac dysfunction and adverse remodeling via mitochondrial biogenesis and SIRT1/PGC-1 $\alpha$ /PI3K/Akt signaling. *J. Cell. Physiol.* 234:23705–23718. <https://doi.org/10.1002/jcp.28939>
- Kuznetsov, A.V., S. Javadov, R. Margreiter, M. Grimm, J. Hagenbuchner, and M.J. Ausserlechner. 2019. The role of mitochondria in the mechanisms of cardiac ischemia-reperfusion injury. *Antioxidants*. 8:454. <https://doi.org/10.3390/antiox8100454>
- Lee, Y., K. Min, E.E. Talbert, A.N. Kavazis, A.J. Smuder, W.T. Willis, and S.K. Powers. 2012. Exercise protects cardiac mitochondria against ischemia-reperfusion injury. *Med. Sci. Sports Exerc.* 44:397–405. <https://doi.org/10.1249/mss.0b013e318231c037>
- Maneeshchote, C., S. Palee, S.C. Chattipakorn, and N. Chattipakorn. 2017. Roles of mitochondrial dynamics modulators in cardiac ischaemia/reperfusion injury. *J. Cell. Mol. Med.* 21:2643–2653. <https://doi.org/10.1111/jcmm.13330>
- Ong, S.-B., S. Subrayan, S.Y. Lim, D.M. Yellon, S.M. Davidson, and D.J. Hausenloy. 2010. Inhibiting mitochondrial fission protects the heart against ischemia/reperfusion injury. *Circulation*. 121:2012–2022. <https://doi.org/10.1161/CIRCULATIONAHA.109.906610>
- Tong, M., D. Zablocki, and J. Sadoshima. 2020. The role of Drp1 in mitophagy and cell death in the heart. *J. Mol. Cell. Cardiol.* 142:138–145. <https://doi.org/10.1016/j.yjmcc.2020.04.015>
- Wang, Y., Q. Liu, J. Cai, P. Wu, D. Wang, Y. Shi, T. Huyen, J. Su, X. Li, Q. Wang, et al. 2022. Emodin prevents renal ischemia-reperfusion injury via suppression of CAMKII/DRP1-mediated mitochondrial fission. *Eur. J. Pharmacol.* 916:174603. <https://doi.org/10.1016/j.ejphar.2021.174603>
- Xiong, W., Z. Ma, D. An, Z. Liu, W. Cai, Y. Bai, Q. Zhan, W. Lai, Q. Zeng, H. Ren, et al. 2019. Mitofusin 2 participates in mitophagy and mitochondrial fusion against angiotensin II-induced cardiomyocyte injury. *Front. Physiol.* 10. <https://doi.org/10.3389/fphys.2019.00411>
- Yuan, J., M. Wang, Y. Pan, M. Liang, Y. Fu, Y. Duan, M. Tang, I. Laher, and S. Li. 2021. The mitochondrial signaling peptide MOTS-c improves myocardial performance during exercise training in rats. *Sci. Rep.* 11:20077. <https://doi.org/10.1038/s41598-021-99568-3>



## Supplemental material

Provided online is Table S1. Table S1 shows the antibody table.

### Animal model and exercise protocol

All animal experiments were performed according to the European Parliament Directive 2010/63/EU and approved by the local ethics committee (No. CEEA-00223, DAP27001). Male Wistar rats (12-wk-old; weight = 225–275 g, Janvier) were randomly assigned to the sedentary control group (Sed) or 5-wk exercise-trained group (ExTr). Moderate exercise training was performed according to a protocol previously described to reduce heart vulnerability to IR [5]. Briefly, rats exercised on a motor-driven treadmill (47300; Ugo Basile, Transforming ideas into instruments) 45 min/day, 5 days/wk for 5 wk at 25 m/min ( $\approx 60\%$  of their MAV). To avoid the acute effects of exercise, rats were sacrificed 24 h after the last exercise training session.

### Ischemia-reperfusion (IR) on isolated perfused heart

Ischemia-reperfusion procedure was performed on isolated hearts, perfused retrogradely with Krebs-Henseleit buffer (KH; 118 mM NaCl, 11 mM D-glucose, 25 mM  $\text{NaHCO}_3$ , 1.25 mM  $\text{CaCl}_2$ , 4.7 mM KCl, 1.2 mM  $\text{MgSO}_4$ , and 1.2 mM  $\text{KH}_2\text{PO}_4$ ; pH 7.4) on a Langendorff apparatus as previously described [10]. Briefly, after stabilization, a total no-flow ischemia in situ was performed for 25 min, followed by 10-min of reperfusion. Hearts were paced at 300 beats/min (Low voltage stimulator, BSL MP35 SS58L, 3V) and a non-compliant balloon was inserted into the left ventricle (LV) to monitor the LV pressure during the entire perfusion. The cardiac functional recovery following IR was determined and LV ischemic contracture time and amplitude were measured at the peak of contracture during ischemia. Hearts tissues were collected and flash-frozen in liquid nitrogen for biochemical experiments or fixed in 2.5% glutaraldehyde/2% paraformaldehyde in a sodium cacodylate buffer (0.1 M) for electron microscopy analysis.

### Transmission electron microscopy

Strips of left ventricular subendocardium were washed and fixed in 2.5% glutaraldehyde/2% paraformaldehyde in a sodium cacodylate buffer (0.1 M) for 2 h at RT and next at 4°C overnight. After rinsing, samples were post-fixed in 1% osmium tetroxide for 1 h, dehydrated through a graded series of ethanol, and embedded in resin. Ultrathin sections of heart tissues were prepared with a diamond knife on a Reichert Ultracut E ultramicrotome and stained with uranyl acetate and lead citrate. Images were photographed under a transmission electron microscope (TEM Hitachi H7800) by randomly selecting photos of longitudinally arranged cardiomyocytes. The mitochondrial area was quantified by manual contouring using ImageJ software, excluding swelled mitochondria. The aspect ratio which reflects the “length to width ratio,” as well as the mitochondrial Feret’s diameter, defined as the longest distance between any two points within the mitochondrion was calculated. Cristae density was evaluated based on the mitochondrial matrix electron density (average greyscale value/pixel) using Image J software. A higher greyscale value indicates a lower cristae density. More than 600 mitochondria per group were analyzed to determine these mitochondrial parameters.

### Statistical analyses

Data were expressed as the mean  $\pm$  SEM or as the median and interquartile range for the violin plots. The normal distribution of the data was tested with the Shapiro–Wilk normality test. Experimental conditions were compared with Student’s t test, analysis of variance (ANOVA) followed by Tukey’s multiple comparisons test, nested analysis of variance (ANOVA), or nested t test. When necessary, non-parametric tests were used (Mann–Whitney test for two groups). A  $P < 0.05$  value was considered statistically significant. The P-value was reported in all the graphs. Statistical analyses were done with GraphPad Prism (8.4.3).